Science of the Total Environment 622–623 (2018) 57–70

Contents lists available at ScienceDirect

Science of the Total Environment

journal homepage: www.elsevier.com/locate/scitotenv

Identification of fine scale and landscape scale drivers of urban aboveground carbon stocks using high-resolution modeling and mapping

Matthew G.E. Mitchell *, Kasper Johansen, Martine Maron, Clive A. McAlpine, Dan Wu, Jonathan R. Rhodes

School of Earth and Environmental Sciences, The University of Queensland, Brisbane, QLD 4072, Australia

HIGHLIGHTS

- Drivers of urban carbon stocks at different spatial scales are largely unknown.
- We modeled urban carbon stocks at high resolution using LiDAR and field data.
- Foliage density above 5 m and canopy height strongly related to aboveground carbon.
- Carbon densities varied strongly with surrounding tree cover extent and clumpiness.
- Managing urban landscape structure important tool to influence urban carbon stocks.

GRAPHICAL ABSTRACT

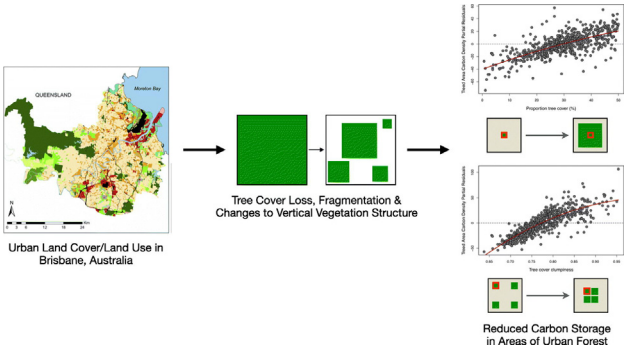
Urban Land Cover/Land Use in Brisbane, Australia
Tree Cover Loss, Fragmentation & Changes to Vertical Vegetation Structure
Reduced Carbon Storage in Areas of Urban Forest

ARTICLE INFO

Article history:
Received 8 September 2017
Received in revised form 22 November 2017
Accepted 22 November 2017
Available online 5 December 2017

Editor: Elena Paoletti

Keywords:
Aboveground carbon storage
LiDAR
Land use/land cover
Urban ecology
Landscape structure
Vegetation structure

ABSTRACT

Urban areas are sources of land use change and CO_2 emissions that contribute to global climate change. Despite this, assessments of urban vegetation carbon stocks often fail to identify important landscape-scale drivers of variation in urban carbon, especially the potential effects of landscape structure variables at different spatial scales. We combined field measurements with Light Detection And Ranging (LiDAR) data to build high-resolution models of woody plant aboveground carbon across the urban portion of Brisbane, Australia, and then identified landscape scale drivers of these carbon stocks. First, we used LiDAR data to quantify the extent and vertical structure of vegetation across the city at high resolution (5×5 m). Next, we paired this data with aboveground carbon measurements at 219 sites to create boosted regression tree models and map aboveground carbon across the city. We then used these maps to determine how spatial variation in land cover/land use and landscape structure affects these carbon stocks. Foliage densities above 5 m height, tree canopy height, and the presence of ground openings had the strongest relationships with aboveground carbon. Using these fine-scale relationships, we estimate that 2.2 ± 0.4 TgC are stored aboveground in the urban portion of Brisbane, with mean densities of 32.6 ± 5.8 MgC ha^{-1} calculated across the entire urban land area, and 110.9 ± 19.7 Mg C ha^{-1} calculated within treed areas. Predicted carbon densities within treed areas showed strong positive relationships with the proportion of surrounding tree cover and how clumped that tree cover was at both 1 km^2 and 1 ha resolutions. Our models predict that even dense urban areas with low tree cover can have high carbon densities at fine scales. We conclude that actions and policies aimed at increasing urban carbon should focus on those areas where urban tree cover is most fragmented.

© 2017 Elsevier B.V. All rights reserved.

* Corresponding author at: Institute for Resources, Environment and Sustainability, The University of British Columbia, Vancouver, British Columbia V6T 1Z4, Canada.
E-mail address: matthew.mitchell@ubc.ca (M.G.E. Mitchell).

http://dx.doi.org/10.1016/j.scitotenv.2017.11.255
0048-9697/© 2017 Elsevier B.V. All rights reserved.

1. Introduction

Urban areas and populations around the world are increasing rapidly in size. While 54% of people today already live in cities (UN, 2014), it is predicted that urban areas will triple in size between 2000 and 2030 (Fragkias et al., 2013; Seto et al., 2012) and that urban populations will increase by 63% from 4 to 6.5 billion by 2050 (UN, 2015). Cities are focal areas of human activities that modify ecosystems and biodiversity (Mcdonald et al., 2008), land cover and landscape structure (Cadenasso et al., 2007), biogeochemical cycles (Grimm et al., 2008), and climate (McCarthy et al., 2010), often at fine spatial scales. In particular, cities are increasingly important for the global carbon cycle as they are locations where human impacts on the global carbon cycle are concentrated (e.g., CO_2 emissions, consumption of primary productivity, Imhoff et al., 2004; Dhakal, 2010) and where the impacts of climate change on human populations will be focused (Hunt and Watkiss, 2011). It is therefore critical to understand how urbanization affects carbon dynamics (Gaston et al., 2013). However, our understanding of carbon dynamics in urban ecosystems, and in particular our ability to identify landscape-scale drivers of urban carbon is underdeveloped (Davies et al., 2011; Hutyra et al., 2011). This prevents the effective planning of urban expansion in order to maintain or increase carbon storage.

Urban areas, while small, can still store significant amounts of carbon below and above the ground (Davies et al., 2011; Davies et al., 2013; Hutyra et al., 2011; Nowak et al., 2013; Raciti et al., 2012). As such, citywide estimates of carbon storage are becoming increasingly common as the need to manage cities and their ecosystems for carbon intensifies. In many cases, urban carbon storage has been found to be higher than previously estimated, sometimes by up to an order of magnitude (Davies et al., 2011). While most of these stores are belowground in soil and plant roots (Churkina et al., 2010; Edmondson et al., 2012), aboveground vegetation also stores significant amounts of carbon. Native vegetation clearing for urban growth is becoming increasingly important for aboveground carbon loss and the global carbon cycle (Churkina et al., 2010) with recent estimates that urban expansion will be the cause of ~5% (1.38 PgC) of deforestation and land use change emissions in the pan-tropics between 2000 and 2030 (Seto et al., 2012). Thus, it is critical to understand how urbanization patterns affect carbon stores.

Urbanization often results in complex patterns of natural ecosystem loss and fragmentation, along with the creation and expansion of new land covers at very fine spatial scales. However, many studies only investigate spatial variation in aboveground carbon across coarse categorizations of land cover (e.g., residential, light urban, heavy urban) (Davies et al., 2011; Hutyra et al., 2011; Raciti et al., 2014), despite knowledge that forest fragmentation and ensuing edge effects are important for carbon stocks in naturally forested landscapes (Pütz et al., 2014; Remy et al., 2016). Unfortunately, these broad categories likely mask important variation in carbon within different land use types (Strohbach and Haase, 2012) and prevent the identification of important landscape-scale drivers of urban carbon, such as changes in landscape structure or urban form. For example, Hutyra et al. (2011) modeled carbon across the Seattle urban area based on five coarse land use classes that may have missed important variation in carbon at finer spatial scales (e.g., Velasco et al., 2013; Raciti et al., 2014). This knowledge gap for urban areas is in part due to the difficulty in obtaining fine-scale land cover and ecological data across entire cities.

One potential way forward is to use remotely sensed imagery and LiDAR data to quantify and model aboveground carbon stocks and landscape structure across cities. Discrete return LiDAR technology employs near-infrared laser pulses fired from an airborne transmitter to measure distances between the transmitter and surface features (Lefsky et al., 2002b). LiDAR pulses reflect off the ground and buildings but also partially reflect off plant parts, such as leaves and stems, providing high-resolution information on the three-dimensional structure of vegetation (Caynes et al., 2016; Davies and Asner, 2014). LiDAR data are increasingly being used to complete high-resolution surveys of vegetation structure over forested areas and cities (Goodwin et al., 2009; Simonson and Allen, 2014; Varhola and Coops, 2013; Alonzo et al., 2015), classify vegetation types (Tooke et al., 2009), identify urban vegetation or street trees (Höfle et al., 2012; Tanhuanpää et al., 2014), and estimate biomass and carbon storage in urban vegetation (Shrestha and Wynne, 2012; Raciti et al., 2014; Alonzo et al., 2016). However, only one study that we are aware of (Godwin et al., 2015) identifies specific landscape-scale drivers of variation in urban carbon stocks that are partially independent of land cover. This gap likely exists due to the extreme fine-scale heterogeneity of land and tree cover in cities (Cadenasso et al., 2007) and difficulty in quantifying landscape structure across urban areas. Thus, there are significant opportunities to use remotely sensed data, including LiDAR, in urban areas to quantify aboveground carbon stores and determine the important landscape-scale drivers of this carbon.

Here, we pair LiDAR-derived measures of vertical vegetation structure with field measures of aboveground woody vegetation carbon in Brisbane, Australia, to: (1) model and map aboveground urban carbon stocks using fine-scale remotely sensed measures of vegetation vertical structure; and (2) provide one of the first determinations of how landscape-scale drivers impact these aboveground urban woody plant carbon stores. These are critical steps to understand how urban carbon stocks will respond to future urban expansion and develop strategies to increase aboveground carbon in cities.

2. Materials and methods

2.1. Study area

Brisbane is a subtropical city of *c.* 1.13 million people located on the eastern coast of Australia (27°28′S, 153°07′E; Fig. 1). The Brisbane Local Government Area (LGA; hereafter referred to as "Brisbane") covers 1378 km^2 and has ~49% tree canopy coverage (Jacobs et al., 2014), with about two-thirds occurring as intact native vegetation (Garden et al., 2007). Annual average minimum and maximum temperatures are 16.3 and 26.5 °C, respectively, with ~2900 h of sunshine and 1006 mm of rain on average (ABOM, 2016). The main upland native vegetation consists of *Eucalyptus* forests dominated by *Eucalyptus signata*, *Corymbia intermedia*, *C. maculata*, *E. crebra*, *Lophostemon confertus*, and *Angophora* spp. (Beckmann et al., 1987). Lowland areas are dominated by open forests of *E. tereticornis*, *E. siderophloia*, *Melaleuca quinquenerva* (broad-leaved paper-bark) and *Casuarina* spp. (she-oak), while mangroves (*Aegiceras corniculatum* and *Avicennia marina*) occur in tidal-influenced saline flats (Beckmann et al., 1987). The urban portion of the city is concentrated along the Brisbane River, with a large conservation area and national park in the northwest. The mean density of dwellings across Brisbane is ~4 dwellings ha^{-1} with an average building height of 6.9 ± 5.2 m. While trees do at times overtop houses in Brisbane, this is not a common occurrence.

Over the last decade, Brisbane City has experienced 2% yr^{-1} population growth rates (QGSO, 2015). This has led to rapid urban expansion of the urban footprint and significant loss of remnant native vegetation and forest cover in the region (Accad and Neldner, 2015). Since 1999, the area of intense land uses (residential, industrial, services, transportation, commercial) has increased by over 3000 ha or 4.4% (DSITI, 2014). Brisbane's population is projected to increase by 15% to 1.3 million people by 2031 (Queensland Government, 2011).

2.2. Overall approach

Our approach first involved measuring aboveground carbon in field plots across an urbanizing gradient. We did this by quantifying tree cover extent and fragmentation across Brisbane and then establishing field plots along this gradient. We then paired this field data with

vertical vegetation structure data derived from LiDAR to build predictive models of aboveground carbon and map carbon across the city. Finally, we used data on land use/land cover, landscape structure (vegetation extent and fragmentation), and urban form across Brisbane to explore how aboveground carbon varies with these factors.

2.3. Vertical vegetation structure

We used 2009 LiDAR data to characterize the vertical vegetation structure (foliage and stems) of tree cover across Brisbane. This data was the most recent LiDAR available at the time of our study. LiDAR data were collected with an airborne ALTM Leica ALS50-II sensor that recorded up to four returns per pulse with a mean of 2 pulses m^{-2}. The accuracy of the data was ±5 cm vertically and ±31 cm horizontally, both at 1 standard deviation. The LiDAR returns were classified into ground and aboveground points by the commercial data provider; we used only the aboveground LiDAR returns in our analysis. We also used a 5 m resolution tree cover layer (presence/absence of vegetation ≥2 m in height) from 2009 obtained from Brisbane City Council (BCC) that was based on LiDAR and satellite image-derived foliage projective cover (Armston et al., 2009), to identify LiDAR returns from treed areas instead of buildings or low vegetation.

Within areas of tree cover, we used methods modified from Miura and Jones (2010) to calculate the relative density of vegetation from the LiDAR data in each of five vertical strata: ≥0.15 to <1, ≥1 to <2, ≥2 to <5, ≥5 to <10, ≥10 m (Tables S1 & S2; Mitchell et al., 2016). We also calculated vertical strata indices from Miura and Jones (2010): openings above ground, openings above low vegetation (0–1 m), presence of understory vegetation (0–1 m), canopy cover, openings above medium vegetation (1–5 m), presence of mid-storey vegetation (1–5 m), presence of high trees (>5 m), and vertically dense canopy of high trees (>5 m) (Tables S1 & S2). In Miura and Jones (2010), the number of LiDAR returns from each stratum is divided by the total number of returns from all strata. In dense canopies, however, few pulses will return to the sensor from lower strata because of interception by vegetation above, despite the presence of dense lower strata. We therefore modified Miura and Jones' (2010) methods by dividing the number of LiDAR returns from each stratum by the total number of returns from that stratum or lower to help account for the number of LiDAR pulses that are able to penetrate to the lower strata (Caynes et al., 2016; Mitchell et al., 2016). We also created a canopy height layer (the top height of the canopy) using the height above the ground below which 95% of the LiDAR vegetation points ≥ 2 m in height were present.

2.4. Land use classification

We used a 1:50,000 land use map of South-east Queensland to determine the location and extent of land use across Brisbane (Fig. 2). This dataset is based on Landsat and SPOT5 satellite imagery, high-resolution orthophotos, aerial photography, ancillary data sets, and field observations from 2011, 2012, and 2013 and has a horizontal accuracy of approximately 25 to 100 m. The dataset classifies land use with a three-level hierarchical structure based on the Australian Land Use and Management Classification (ALUMC) Version 8 (ABARES, 2016); we used the second level of the hierarchy for our analysis.

2.5. Aboveground biomass field sampling

We measured aboveground biomass in woody vegetation at 219 sites across Brisbane from December 2014 to April 2015. Our sampling scheme was designed to span the range of tree cover extent and fragmentation present across the city, as these variables have been found to be important drivers of vertical vegetation structure in Brisbane (Mitchell et al., 2016). We first used the 5 m resolution tree cover dataset described earlier to quantify tree cover extent (tree cover proportion) and tree cover fragmentation (perimeter-to-area ratio) in a

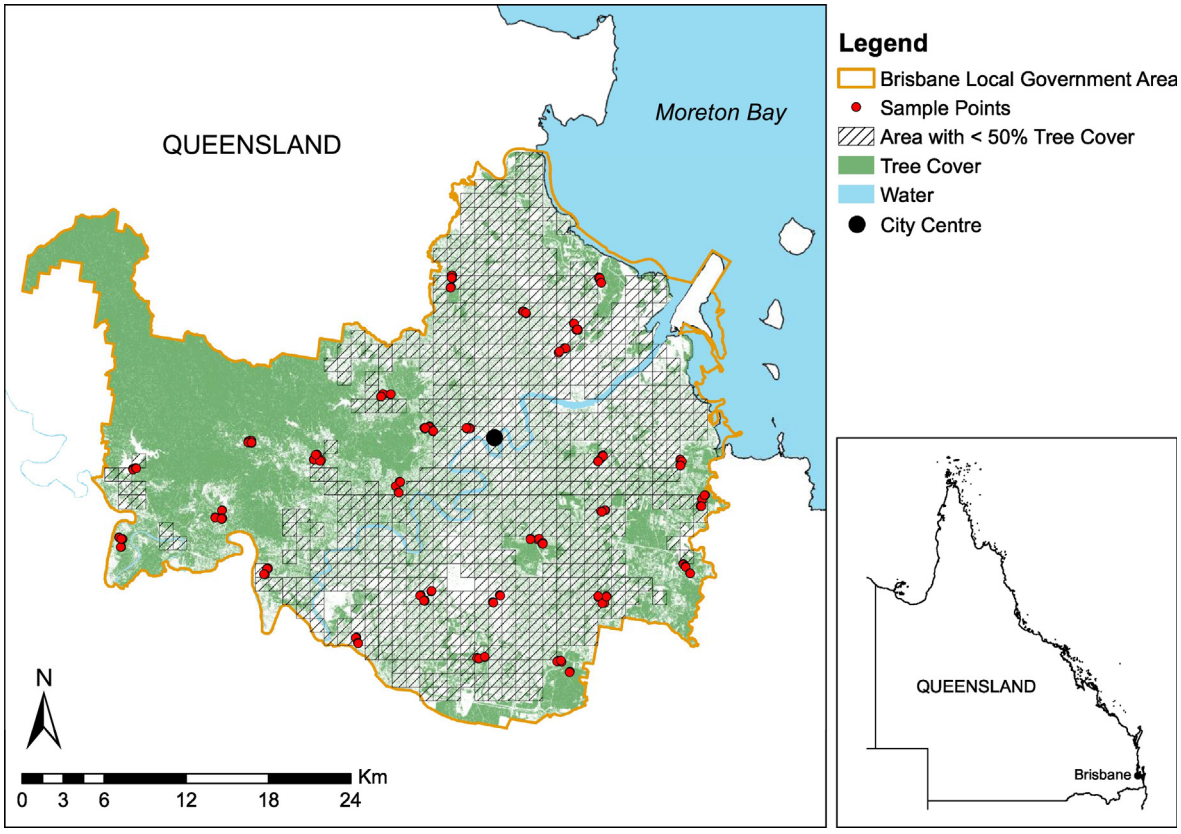

Fig. 1. Sample locations overlaid on a tree cover map of Brisbane. Sample locations were stratified across tree cover extent and fragmentation at a 1 km^2 resolution, tree cover extent at a 1 ha resolution, and tree height at a 25 m^2 resolution. The hatched area shows the urban area of Brisbane with <50% tree cover.

1 km^2 grid across the entire Brisbane LGA, as well as tree cover extent in a finer 1 ha grid. These two nested spatial scales were used to capture both the broad- and fine-scale variation in tree cover across the city (i.e., 1 km^2 cells with very little tree cover often included 1 ha cells with high tree cover, and vice versa). We then stratified our sampling locations across (1) tree cover extent and fragmentation at a 1 km^2 resolution; (2) tree cover extent at a 1 ha resolution; and (3) tree height at a 25 m^2 resolution (Fig. S1). A full description of our sampling scheme can be found in the Appendix S1 and Fig. S1.

We used 25 m^2 sample plots (5 × 5 m) in order to match the resolution of our vegetation structure data, minimize the number of sample plots that crossed property boundaries, and be consistent with other similar studies of urban aboveground carbon storage (e.g., Davies et al., 2011). Plot centers were located using a Garmin GPSmap 60CSx GPS unit (Olathe, Kansas, USA) that generally had a 2–5 m horizontal error. We supplemented GPS locations using detailed maps of vertical vegetation structure, streets, and property boundaries to locate plot centers, although this was more difficult in heavily treed areas where obvious landmarks were absent.

2.6. Aboveground carbon estimates

Diameters of all trees and shrub stems >2 m in height and 0.5 cm diameter at breast height (DBH; 1.37 m) were measured in each plot to the nearest 0.1 cm. Tree heights to the nearest 0.1 m were also measured in the field, using a Nikon Forestry 550 Laser Rangefinder (Sydney, NSW, Australia), a clinometer and meter tape, or directly using a meter tape for small trees and shrubs. All stems were identified to species if possible (82.7% of all stems), but due to difficulty identifying some ornamental and hybrid *Acacia*, *Banksia*, *Melaleuca*, *Eucalyptus*, and *Leptospermum* species, along with many exotic species, 13.5% of measured stems could only be identified to genus. Only 3.8% of all stems could not be identified (unknown species or standing dead stems).

Aboveground woody biomass was calculated using allometric equations from the literature that relate either DBH or DBH and tree height to dry mass (Table S3). Species-specific equations were used if available, otherwise genus, family, or as a last resort a widely-used generic tropical dry forest equation (Chave et al., 2005) were substituted. Where multiple allometric equations were available, we averaged the results of up to a maximum of six different equations to create a generalized result (McHale et al., 2009). For mangrove trees, we created a generalized equation that averaged 13 different mangrove-specific allometric equations. The generic tropical dry forest equation requires species- or genus-specific wood density estimates. We sourced these from the World Agroforestry Centre (ICRAF) Tree Functional Attributes and Ecological Database (http://db.worldagroforestry.org). Where genus or species-level densities were not available, or where stems could not be identified, we used the mean wood density value of all other stems in our sample. For standing dead trees, we reduced the live mass result by 3.0% to adjust for loss of leaves (Nowak, 1993). Where required, we corrected our back-transformation of logarithm-transformed allometric equations (Baskerville, 1972); see Appendix S2 for a full description of these corrections. Some studies have also used corrected aboveground biomass estimates for urban trees, assuming that most allometric equations that are based on trees in forest ecosystems will overestimate aboveground biomass in urban settings (Hutyra et al., 2011; Nowak, 1994). However, this technique has been recently criticized and could lead to significant underestimates of urban carbon (McHale et al., 2009). Because our plots spanned both urban and more forested areas and our allometric equations were from both forest and plantation systems, we decided against correcting our estimates this way. Finally, we assumed that 48% of the aboveground dry mass of each tree was carbon (Asner et al., 2010).

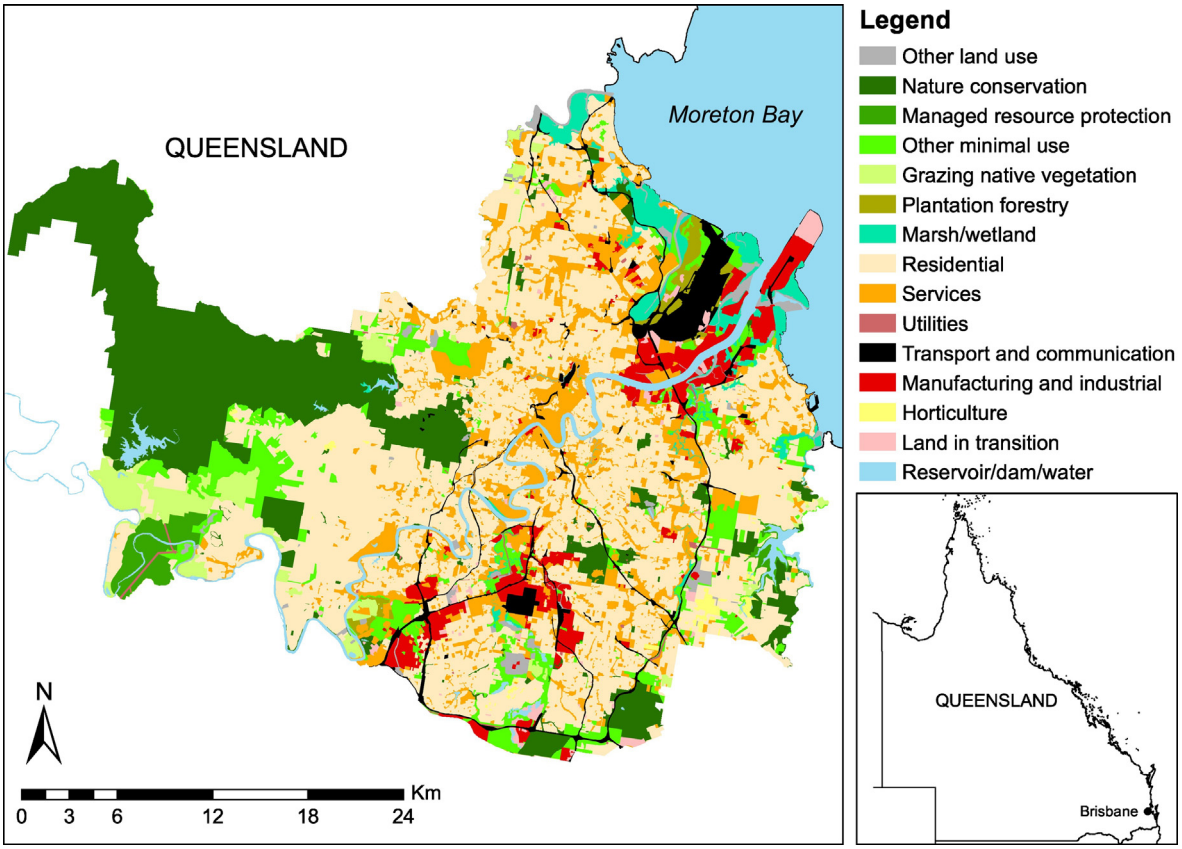

Fig. 2. Land use/land cover across the Brisbane LGA.

2.7. Modeling aboveground C across Brisbane

We used boosted regression trees (BRTs; Hastie et al., 2011) to model how aboveground woody plant carbon stores vary with vegetation vertical structure across Brisbane. BRTs are a form of machine learning based on regression trees and boosting that combine multiple simple models to improve model prediction (Elith et al., 2008). They fit a large ensemble of regression tree models that are then combined to provide better estimates of the response. Their advantages are that they are relatively insensitive to outliers, irrelevant predictors, or correlated predictor variables, and they can readily include complex interactions between the predictor variables (Buston and Elith, 2011; Leathwick et al., 2006). Potential disadvantages are that BRTs can be more difficult to interpret and scrutinize, that they fail to provide a single simple model result, and that they commonly overfit ecological data and demonstrate noisy fitted functions (Elith et al., 2008). However, these potential problems have been found to not affect the predictive power of BRTs (Elith et al., 2008) and BRTs repeatedly outperform traditional modeling techniques (e.g., Garćia-Gutiérrez et al., 2015; Lieb et al., 2016). BRTs utilizing remotely sensed or LiDAR data have also been used by other authors to assess forest biomass and aboveground carbon (e.g., Razakamanarivo et al., 2011; Li et al., 2014; Ma et al., 2017) and tree species abundance (e.g., van Ewijk et al., 2014). We created BRTs with the 'gbm' package version 2.1.1 in R (Ridgeway, 2015) and custom code provided in Elith et al. (2008). As a first step, we created BRTs of aboveground C using our 14 vegetation structure variables (Section 2.3) plus other spatial datasets of variables with high potential to be related to aboveground carbon stocks: NDVI, foliage projective cover, elevation, and aspect (Tables S1 & S2; Figs. S2–S8). We used a 'learning rate' of 0.004 to ensure that at least 1000 regression trees were fit as recommended by Elith et al. (2008), and a 'tree complexity' value of 6. These values gave our models the greatest explanatory and predictive power when compared to a range of other values, as determined by the proportion of deviance they explained. Deviance is a measure analogous to variance in general linear models, but is generalized to allow application to models fit using maximum likelihood. To control for over-fitting, we used 10-fold cross-validation to progressively test each model on withheld subsets of the data. Twenty percent of the data was withheld for cross-validation. Next, we simplified our BRT models using methods similar to backward selection in regression to remove unimportant variables (Elith et al., 2008). To quantify variation in model results, we bootstrapped our simplified BRT model 300 times. We then used these 300 simplified BRT models in R to predict aboveground carbon values at a 25 m^2 resolution across the urban area of Brisbane where tree cover at a 1 km^2 resolution was <50% (Fig. 1). We focused on this subset area of the Brisbane LGA to exclude the more rural and protected area portions of the city that are not as strongly influenced by urban land use change, and thus ensure that our results were comparable to other urban carbon studies. From our predicted datasets, we calculated mean values and the range of BRT predictions in order to estimate the percentage uncertainty in our carbon storage values.

2.8. Variation in aboveground C across land use/land cover categories

We next identified how predicted aboveground carbon storage values from the BRT analysis varied with land use/land cover across the urban portion of Brisbane. We calculated mean carbon density values for each land use/land cover category in two ways: per hectare of total land area, and per hectare of tree cover. In the first method, we summed the total predicted aboveground carbon in each land use/land cover category and then divided this by the entire areal surface of that land use/land cover category. This provided a measure of overall carbon density. In the second method, we summed the total predicted aboveground carbon in each land use/land cover category and then divided this by the area of tree cover within that land use/land cover category. This provides a measure of carbon density exclusively for treed areas that takes into account the amount of forest loss and land clearing present in each land use/land cover category.

2.9. Identifying landscape-scale drivers of aboveground C

We used spatial autoregressive modeling (SAR) and multimodel inference to investigate which urban landscape structure variables best explain the predicted carbon densities across Brisbane. First, we calculated mean carbon densities at two spatial resolutions (1 km^2 and 1 ha) from the original 25 m^2 resolution predicted carbon values. We chose these two resolutions as they provide standard and consistent spatial units of analysis, are large enough to allow for the calculation of important landscape structure variables, and are readily comparable to previous urban and forest ecology studies. Next, at the same two spatial resolutions, we created and compared competing four-variable models of urban form (dwelling density, mean lot size, road density, and proportion parkland; Fig. S7) and landscape structure variables based on urban tree cover (tree cover proportion, tree cover clumpiness, tree cover perimeter:area ratio, and mean tree cover patch size or number of patches; Fig. S8) calculated using Fragstats 4.2 (McGarigal et al., 2012), as well as combined four-variable models of urban form and landscape structure. These combined models were identified by creating every possible four-variable model using the 'MuMIn' package (Bartón, 2013) in R and then choosing the best model based on the corrected Akaike's Information Criterion (AICc).

We used SAR to account for spatial autocorrelation that can make model standard errors unreliable if methods like ordinary least squares regression (OLS) are used (Dormann et al., 2007). SAR models were run using the 'spdep' package (Bivand et al., 2015) in R. In each SAR, we defined neighbouring cells as those with centroids <1500 m from each other for the 1 km^2 analysis, and <150 m for the 1 ha analysis (i.e., first-order neighborhoods with queen contiguity). We created all SAR models using all three possible types of neighbourhood matrices (lagged, error, and mixed) and selected the best model based on AICc. Where appropriate, dependent variables were $\log_e$ transformed to improve normality and meet modeling assumptions. All explanatory variables were standardized by centering them on zero and dividing by 2 standard deviations using the '*rescale*' function in the 'arm' package (Gelman et al., 2013) of R and we used second-order polynomial terms to model nonlinear relationships. Colinearity between explanatory variables was calculated using variance inflation factors (VIFs). All VIFs were <1.9, indicating minimal issues. The ability of the models to account for spatial autocorrelation was evaluated using Moran's *I* values, semivariograms, and maps of model residuals. Model fit of the full SAR model was evaluated with pseudo-R^2 values (Nagelkerke, 1991) using the log-likelihood values of the full SAR model and an identical OLS model without any explanatory variables. For model fit of just the non-spatial portion of each SAR model, we calculated pseudo-R^2 values using a null SAR model that accounted for spatial autocorrelation but lacking any explanatory variables. This second R^2 evaluated the model fit of the explanatory variables independent of any spatial lag or error terms.

3. Results

3.1. Field results

We measured 1197 stems of 127 tree and shrub species containing an estimated 39,638 kg of carbon across 219 sampling plots (Fig. S9). Twenty of our plots did not contain any stems. Mean stem diameter was 9.0 ± 10.2 cm (mean ± 1 s.d.) while mean height was 5.9 ± 3.4 m. Maximum stem diameter was 83.0 cm for a brush cypress (*Callitris macleayana*) growing at the edge of a private, peri-urban residential property, while the tallest stem was a 30.5 m lemon-scented gum (*Corymbia citriodora*) in a relatively undisturbed rural forest on

private land. Most stems had diameters <29.5 cm (95%) and heights <11.9 m (95%; Fig. S10). Large stems >20 cm in diameter, while uncommon, stored a large amount (75%) of the observed C, while the majority of C was stored in stems >5 cm in diameter (95% of C; Fig. S10). Similarly, stems >10 m in height were relatively rare but stored 60% of measured C while stems >5 m in height stored the majority of C (95%).

Field estimates of vegetation cover for different vertical strata at each sample point showed positive correlation with our remotely sensed LiDAR vertical vegetation structure estimates (2–5 m vegetation: *Pearson corr.* = 0.3; 5–10 m vegetation: *Pearson corr.* = 0.5; >10 m vegetation: *Pearson corr.* = 0.7). These positive correlations were present despite the difficulty in defining vertical strata and vegetation cover values visually (Kennedy and Addison, 1987) and the ~6 years that had passed between LiDAR acquisition and field sampling. This gives us some confidence that this time lag is unlikely to be a major issue for our carbon models and results.

3.2. Modeling of aboveground carbon

Five remotely sensed vegetation vertical structure variables were retained in our BRT model for aboveground C (Fig. 3). The bootstrapped models ($n = 300$) explained on average 63.8 ± 1.9% (mean ± 1 s.d.) of the deviance in the training data (the ability of the BRTs to explain observed data) and 31.2 ± 2.5% of the deviance using cross-validation (the ability of the BRTs to predict left-out data). These values of explained deviance indicated that our BRT model was overfitting the training data, which is a common situation with BRTs. However, unlike normal statistical modeling, previous studies have found that this situation generally does not affect the ability of the BRT models to predict to independent data (Elith et al., 2008). Vegetation cover above 10 m in height and vertically dense vegetation >5 m in height contributed most to our model (29.2 and 24.7% respectively). For both the >10 m and dense vegetation >5 m strata, aboveground C generally increased as vegetation cover increased, but decreased slightly when vegetation cover above 10 m was between 30 and 40% (Fig. 3a,b). Canopy height contributed 19.3% to our model, with aboveground C steadily increasing with canopy height, especially up to 20 m. Finally, two variables, openings above ground (18.5% contribution) and vegetation cover between 1 and 5 m in height (8.3% contribution), corresponded to rapid decreases in aboveground C at low values (0–5%; Fig. 3d,e).

Our BRTs predict that 2.2 ± 0.4 TgC (million metric tons of C) are stored in aboveground woody vegetation within the urban portion of the Brisbane LGA. This equates to an average of 32.6 ± 5.8 MgC ha^{-1} across the total land area of this portion of the city (Figs. 4a & S11) and 110.9 ± 19.7 MgC ha^{-1} within just the treed areas (Figs. 4b & S11). Within this urban area of Brisbane, nearly half of the stored C (47.1%) is predicted to be stored within residential areas, almost a quarter in service areas (22.6%), and disproportionately 6.5% in nature conservation areas, even though they only cover 1.6% of the urban portion of Brisbane (Table 1).

3.3. Predicted aboveground carbon across land use categories

Carbon densities varied greatly across land use categories throughout the city and decreased significantly as land use intensity increased, although this variation was reduced when carbon densities were calculated solely across treed areas (Fig. 5). Across Brisbane's urban area, nature conservation, resource protection, plantation forests, and other minimal use land uses showed the highest overall C densities (all above 68 MgC ha^{-1}) while more disturbed land use categories including land in transition, horticulture, transportation, and industrial areas all had C densities below 30 MgC ha^{-1} (Fig. 5; Table 1). Residential areas, which make up the largest portion of the urban portion of Brisbane (51.3%), had a C density of ~30 MgC ha^{-1}. When just treed areas were considered, nature conservation areas had C densities of 160 MgC ha^{-1}, while other areas of low land use intensity had treed area C densities >100 MgC ha^{-1} (e.g., resource protection, plantation forests, other minimal use areas, marsh/wetland, services, utilities, and native vegetation grazing; Fig. 5, Table 1). Treed areas in residential areas had mean C densities of ~95 MgC ha^{-1}, while treed areas within areas of high land use intensity, including industrial, transportation, and horticulture all had C densities above 88 MgC ha^{-1}. Importantly, the differences in C densities across different land uses in Brisbane were smaller when just treed-area C densities were considered (Fig. 5).

3.4. Broad scale drivers of predicted aboveground carbon

Most of the variation in carbon, calculated both across the total land area and only within treed areas, was strongly correlated with landscape structure. SAR models containing only landscape structure variables performed significantly better than urban form models at both 1 km^2 and 1 ha resolutions in every case (Table 2). Similarly, the best combined models included predominantly landscape structure variables, in addition to the proportion of parkland present (Table 3). The best combined and landscape structure models of total land area C density at both spatial resolutions showed excellent fit, with all $R^2 \geq 0.75$ (range: 0.77–0.89), although model fit was lower for the 1 ha analysis. Model fit for treed-area C density in each case was lower, but still high with all $R^2 \geq 0.40$ (range: 0.42–0.65).

Each of the best combined models included tree cover proportion and clumpiness (Table 3). Mean patch size and proportion parkland were also important at the 1 km^2 resolution, while the number of patches was included in each best model at the 1 ha resolution. In all cases analyzed (i.e., 1 km or 1 ha resolutions), both total area C and treed area C densities increased with tree cover and tree cover clumpiness (Fig. 6) and decreased with mean tree cover patch size across the urban area of Brisbane (Fig. S12), although these latter relationships were much weaker.

4. Discussion

Rapid urbanization has the potential to substantially affect carbon stocks worldwide, with impacts increasing as the size of cities and urban areas continue to grow (Seto et al., 2012). There is a critical need to better understand the drivers of urban carbon stocks at multiple scales, especially across gradients of urbanization. Our study offers strong evidence that urban landscape structure – the patterns created by vegetation removal and creation across cities – is an important driver of urban carbon stocks at fine and coarse spatial scales due to its effects on vertical vegetation structure. In addition, our results add to the accumulating evidence that aboveground urban carbon stocks, at least a fine spatial scales, can be comparable to those in natural or managed forest systems (Hutyra et al., 2011; Nowak and Crane, 2002; Raciti et al., 2012). These results have important implications for our understanding of how urbanization will impact carbon and how cities should be designed and managed in order to maintain and maximize carbon stores.

4.1. Relationships between vegetation structure and urban aboveground carbon

The strong relationship we observed between canopy height as measured by LiDAR and aboveground woody plant carbon reflects a widespread positive relationship that has been seen in a number of similar tropical forest studies (e.g., Asner et al., 2010, 2014). Similarly, a relationship between vegetation height (shrubs, tall shrubs, versus trees) was seen in Leicester, UK (Davies et al., 2011). However, our analysis also identified a number of other important vegetation structure variables that have not been commonly used in analyses of aboveground carbon, including vegetation density at different heights above ground, as well as the presence of openings above ground. Relationships between these variables and aboveground woody plant carbon were as expected, with aboveground carbon generally increasing with

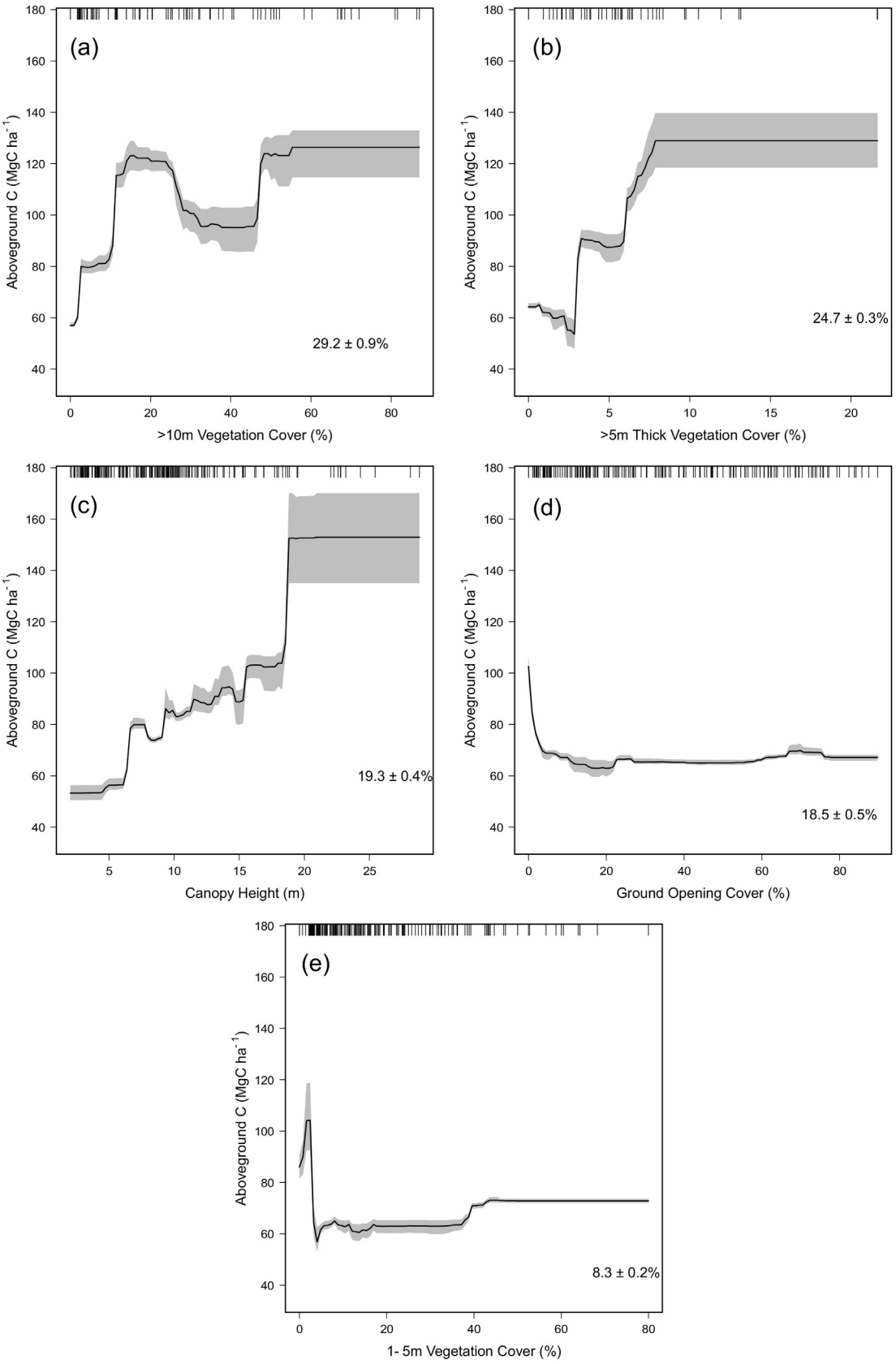

Fig. 3. Aboveground carbon density partial dependence plots from boosted regression trees for the five most influential variables that predict aboveground carbon densities within treed vegetation. Fitted lines represent the mean estimate (*black*) and range of values (*grey*) based on 300 bootstrap replicates. Rug plots inside the top of the plots show the distribution of field samples on the *X*-axis.

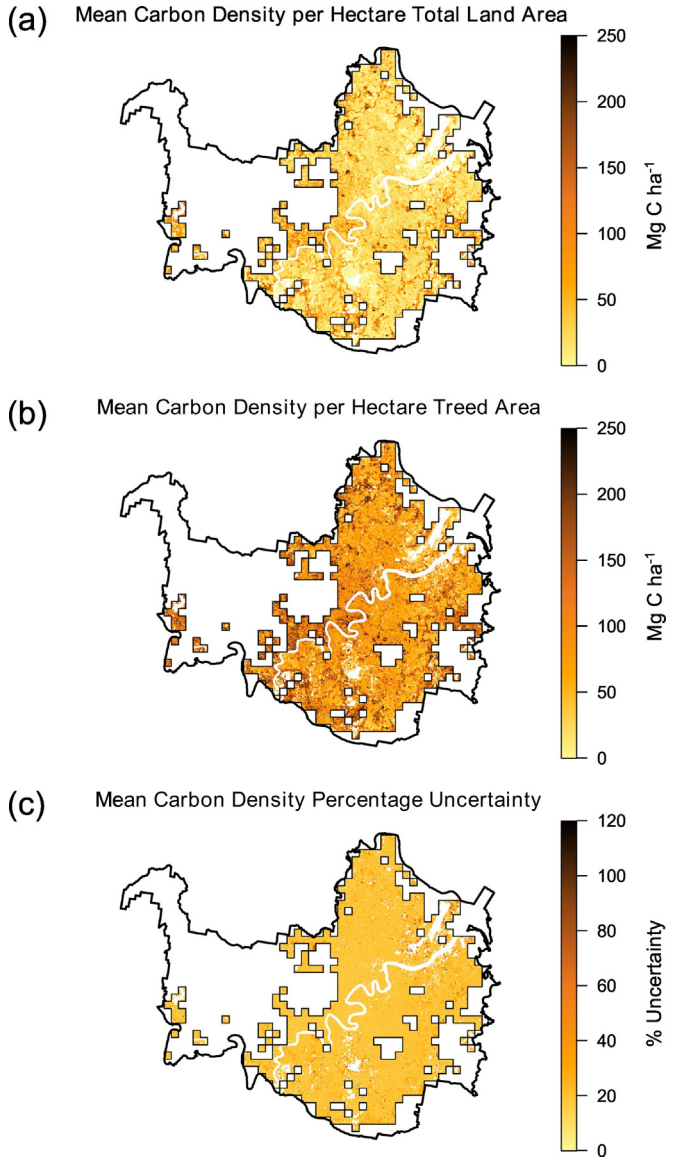

Fig. 4. (a,b) Predicted aboveground carbon densities (MgC ha^{-1}) and (c) percentage uncertainty in these estimates for the urban area of Brisbane based on vegetation structure metrics from LiDAR data and boosted regression tree results. Mean aboveground carbon density is calculated (a) across total land area, and (b) across only treed areas. White areas are where no estimate was possible due to the presence of water or lack of LiDAR data.

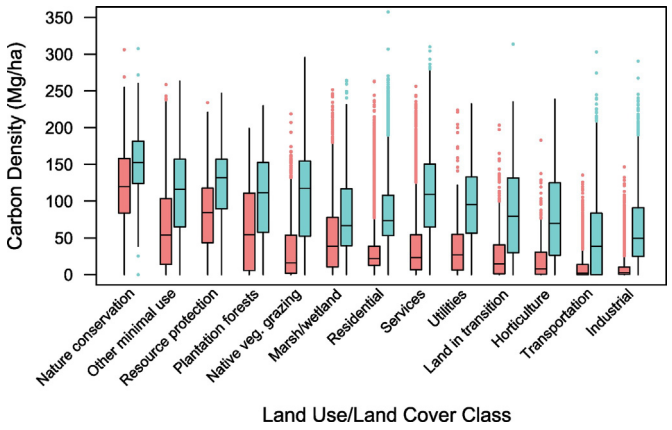

Fig. 5. Predicted aboveground carbon densities (MgC ha^{-1}) at a 1 ha resolution for the thirteen most extensive land use classes in the urban portion of Brisbane (area with <50% tree cover). Predictions are based on vegetation structure metrics from LiDAR data and boosted regression tree results. Mean aboveground carbon densities are calculated across the total land area of each land use class (*red bars*) and across only treed areas (*blue bars*). Boxplots show the median (*middle bar*), first and third quartile (*box*), 1.5 interquartile range (*whiskers*), and outliers (*points*).

vegetation cover (Lefsky et al., 2002a) but decreasing as openings became more prevalent. Identification of strong relationships between vegetation density at different heights and aboveground carbon in our study suggests that incorporating these variables into aboveground carbon models, both across urban landscapes as well as other forested ecosystems, would be an important improvement over existing methods.

Our models of aboveground woody plant carbon showed reasonable explanatory (64%) and predictive (31%) power, but could not match the predictive power of similar studies across tropical and temperate forests (74–94%), although these studies modeled carbon at coarser resolutions (0.1 to 0.05 ha) than our study (e.g., Asner et al., 2010, 2014; Drake et al., 2002; Lefsky et al., 2002a). We expected that the higher variability in carbon densities at the finer resolutions at which we applied our models would lead to lower predictive power. Given the nature of LiDAR data, at finer spatial resolutions fewer LiDAR pulses are available to quantify vegetation structural variables and provide ground returns, which could lead to increased uncertainty in these measures (e.g., vegetation cover and canopy openings). High tree canopy densities can also contribute to this when they prevent LiDAR pulses from returning to the sensor. While our LiDAR data had a point density of 2 pulses m^{-2}, other work has suggested that higher densities are required for some measures of vegetation vertical structure such as Leaf Area Index and carbon storage (Alonzo et al., 2016; Richardson et al., 2009), although at least one study found no difference in results when using either 22 or 2 pulses m^{-2} (Alonzo et al., 2015). We also expected that the

Table 1
Predicted aboveground carbon densities in different land use categories across the urban portion of the Brisbane LGA.

Land use	Total area (ha)	Total area carbon density (MgC ha^{-1})	Treed area carbon density (MgC ha^{-1})	Tree cover	Total carbon (GgC)
Nature conservation	1090 (1.6%)	131.3 ± 23.3	160.0 ± 28.4	82.1%	143 (6.5%)
Resource protection	278 (0.4%)	84.2 ± 15.4	133.1 ± 24.3	63.2%	23 (1.0%)
Plantation forests	392 (0.6%)	69.1 ± 12.1	128.0 ± 22.5	54.0%	27 (1.2%)
Other minimal use	2735 (4.1%)	68.2 ± 12.1	137.2 ± 24.3	49.7%	187 (8.5%)
Marsh/wetland	1696 (2.6%)	54.7 ± 10.0	100.8 ± 18.6	54.2%	93 (4.2%)
Services	12,487 (18.8%)	39.9 ± 6.8	139.9 ± 24.1	28.5%	498 (22.6%)
Utilities	182 (0.3%)	33.9 ± 6.0	113.4 ± 20.2	29.8%	6 (0.3%)
Native veg. grazing	1329 (2.0%)	32.5 ± 6.0	136.6 ± 25.0	23.8%	43 (2.0%)
Residential	34,004 (51.3%)	30.5 ± 5.4	95.0 ± 17.0	32.1%	1037 (47.1%)
Land in transition	663 (1.0%)	26.7 ± 4.8	114.7 ± 20.8	23.3%	18 (0.8%)
Horticulture	383 (0.6%)	14.3 ± 2.6	97.3 ± 17.3	14.7%	5 (0.2%)
Transportation	3311 (5.0%)	8.1 ± 1.5	88.7 ± 16.7	9.1%	27 (1.2%)
Industrial	4474 (6.7%)	7.2 ± 1.4	95.4 ± 11.5	7.6%	32 (1.5%)

Table 2
Spatial autoregressive (SAR) model results, including model corrected Akaike Information Criterion (AICc) values, for total land area and treed area carbon densities across the urban area of Brisbane at 1 km^2 and 1 ha spatial resolutions.

Dependent variable	Model	SAR model type	AICc	ΔAICc	R^2 full SAR model	R^2 partial model	SAR Moran's *I*
1 km^2 resolution							
Total area C	Best combined	Mixed	3802	–	0.93	0.89	−0.008
	Landscape str.	Mixed	3833	31	0.93	0.88	−0.007
	Urban form	Error	5081	1279	0.47	0.15	−0.024
Treed area C	Best combined	Mixed	5177	–	0.76	0.65	−0.018
	Landscape str.	Mixed	5211	34	0.75	0.63	0.001
	Urban form	Mixed	5608	431	0.53	0.31	−0.027
1 ha resolution							
Total area C[a]	Best combined	Mixed	77,978	–	0.87	0.77	−0.032
	Landscape str.	Mixed	77,978	–	0.87	0.77	−0.032
	Urban form	Mixed	160,850	82,872	0.49	0.06	−0.027
Treed area C[a]	Best combined	Mixed	31,459	–	0.67	0.43	−0.041
	Landscape str.	Mixed	31,772	313	0.67	0.42	−0.029
	Urban form	Mixed	58,356	26,897	0.48	0.09	−0.031

[a] Variable was $\log_e$ transformed to improve normality and meet modeling assumptions.

predictive power of LiDAR carbon models will necessarily be lower in urban areas given the high variability in land management, history, tree species, and biophysical conditions (Cadenasso et al., 2007). The lag between LiDAR acquisition (2009) and field sampling (2014–15) in our study may also have contributed to our lower predictive power, as the urban forests in Brisbane regrew, were replaced, or were cleared in some places. However, the positive correlations between our field measurements of vegetation structure and the LiDAR-derived metrics suggest that this may not have been a significant issue. In any case, the spatial patterns of carbon storage across Brisbane estimated here are likely to be more robust to these issues than absolute values. Thus, our main results which focused on the relationships between landscape-scale variables and urban carbon stocks are unlikely to have been significantly affected by these issues.

Regardless, there remain significant opportunities to investigate if including different LiDAR-derived vegetation structure metrics (e.g., Jaskierniak et al., 2011; Lovell et al., 2003), or additional urban form (e.g., street density, impervious cover) and socioeconomic (e.g., income, neighbourhood age) variables will improve models of urban carbon. New methods are also being developed to combine vegetation and tree species information derived from high-resolution satellite imagery (e.g., Tooke et al., 2009) with LiDAR canopy height data to model urban carbon (Ediriweera et al., 2014; Tigges et al., 2017). These types of methods offer an important way forward to potentially increase the accuracy of urban carbon models.

4.2. Landscape-scale drivers of urban aboveground carbon stocks

Our analysis of Brisbane found that carbon stocks within different land uses/covers were highly variable (Fig. 5) and that carbon densities varied most with changes to urban landscape structure, and to a lesser extent urban form (Fig. 6; Table 2). Carbon densities across the entire urban Brisbane area, and most importantly within treed areas, showed strong positive relationships with the amount of tree cover present and the clumpiness of tree cover patches in the surrounding area (1 km^2 or 1 ha). While spatial variation in tree cover was the strongest driver of carbon densities when calculated across the entire land area of the urban portion of Brisbane (Fig. 6a), surprisingly, we also observed significant decreases in carbon densities within treed areas when forest cover in the surrounding area was reduced or more fragmented (Fig. 6d,e). In other words, reduction in tree cover had a predictable negative effect on total carbon stores through direct loss of vegetation, but also a strong indirect negative effect by simplifying vegetation structure when smaller and more fragmented patches of vegetation were present. While our data is correlative, it suggests that fragmentation of tree cover across gradients of urbanization can drive additional carbon loss in urban areas.

In forest ecosystems, fragmentation of forests into smaller patches often leads to decreased carbon storage. In tropical rainforests, forest fragmentation and increased edge effects drive changes in vegetation structure that can lead to lower aboveground carbon stores (Chaplin-Kramer et al., 2015; Pütz et al., 2014). In temperate forests, there is a lack of similar studies, although some contrasting results have been seen (Remy et al., 2016; Ziter et al., 2014). While similar effects have not been shown in urban settings, our results suggest that comparable changes may also be driving change in aboveground urban carbon stocks. The main mechanisms behind these types of effects in natural ecosystems are thought to be changes in light and moisture regimes associated with increased forest edges that drive changes in vegetation structure (Harper et al., 2005), and shifts in plant species composition due to edge effects that then alter vegetation structure (Damschen et al., 2006). While studies of similar mechanisms in urban settings are lacking, recent evidence from Brisbane using LiDAR data to quantify the drivers of vegetation vertical structure suggests that tree cover loss and fragmentation are associated with lower foliage projective cover, canopy heights, and vegetation vertical structural complexity (Mitchell et al., 2016). However, human disturbance and active management of vegetation are also likely to have important effects

Table 3
Summary of explanatory variables included in the best combined SAR models.

Model	Variables and standardized polynomial model coefficients in best combined model[a,b]
1 km^2 resolution	
Total area C	% Tree cover (30.7, 4.9), clumpiness (11.6, −4.4), patch area (−1.3, 0.0), proportion parkland (−1.4, −0.6)
Treed area C	% Tree cover (24.5, −3.1), clumpiness (44.1, −9.6), patch area (−7.1, 0.5), proportion parkland (−4.2, −1.8)
1 ha resolution	
Total area C[c]	% Tree cover (2.7, −1.0), clumpiness (1.0, 0.6), # patches (0.6, −0.6), perimeter:area ratio (−0.3, <0.1)
Treed area C[c]	% Tree cover (0.6, <0.1), clumpiness (0.9, 0.5), proportion parkland (0.2, −0.1), # patches (0.1, −0.2)

[a] Order of variables does not imply relative strengths of relationships.
[b] Coefficients in brackets refer to first-order and second-order polynomials.
[c] Variable was $\log_e$ transformed to improve normality and meet modeling assumptions.

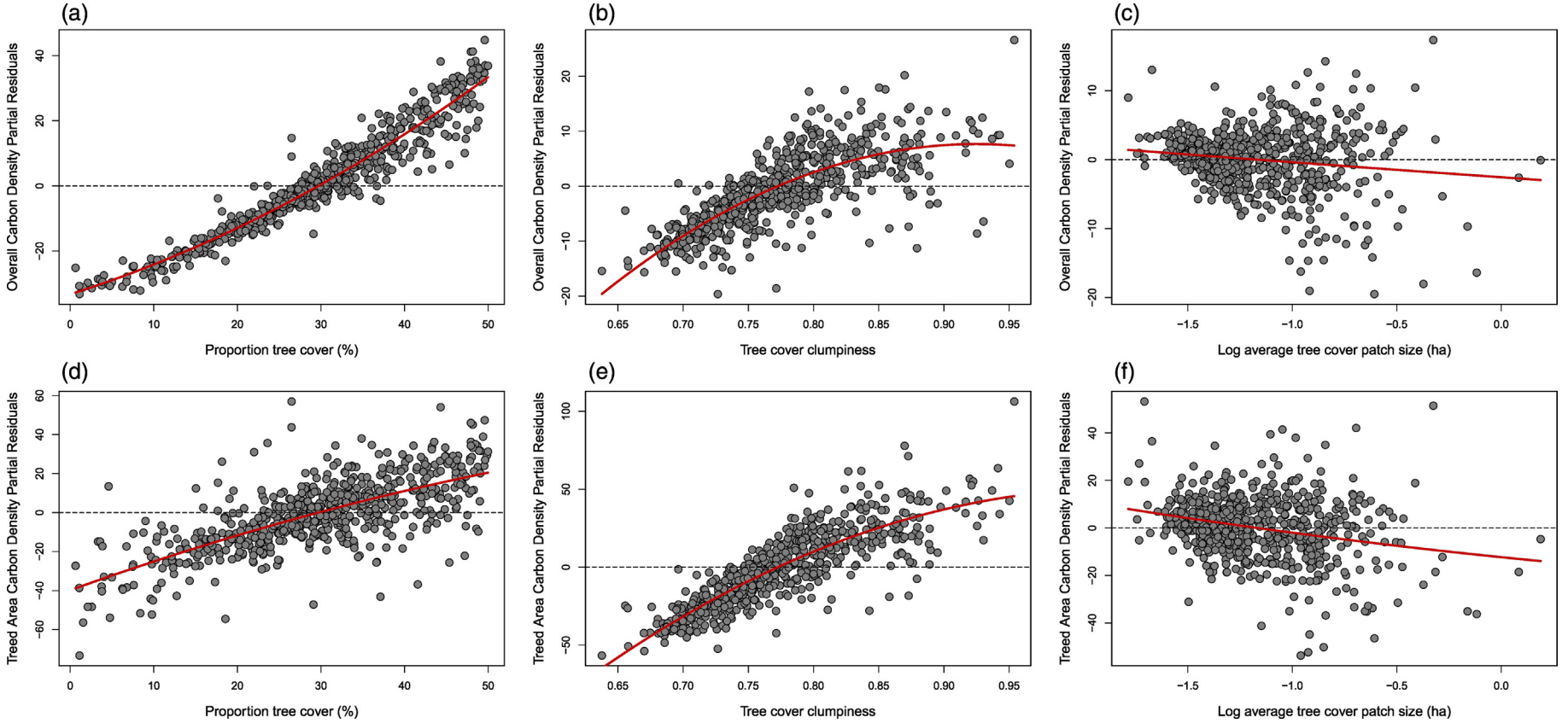

Fig. 6. Partial effects of landscape structure on (a–c) total area carbon densities and (d–f) treed area carbon densities at a 1 km^2 spatial resolution across the urban area of Brisbane. *Y*-values were calculated by adding the residuals from each best combined model (see Tables 2 & 3) to the product of each explanatory variable in question (i.e., proportion tree cover, tree cover clumpiness, or tree cover patch size) and the slope estimate for carbon density.

on vegetation structure in urban areas (Trombulak and Frissell, 2000) and how these activities interact with or alter edge dynamics in urban forests is unknown. For example, management for recreation (e.g., shade trees), the removal of hazard trees, or the introduction of exotic species could all impact urban vegetation vertical structure and hence carbon stores. Historical legacies and spatially non-random human activities across Brisbane also likely contributed to our landscape-scale findings. For example, areas with larger trees and therefore larger carbon stocks may have been prioritized for conservation as urban parks, which would limit forest fragmentation in those areas. Similarly, secondary tree regrowth following urban development might dominate those areas that are most fragmented in Brisbane, resulting in the observed relationships between landscape structure and aboveground carbon stocks.

4.3. Size of predicted urban aboveground carbon stocks

Carbon stocks in cities have generally been assumed to be small relative to those of forested ecosystems (Churkina et al., 2010). However, there is growing evidence that urban carbon stocks, at least those within forested land covers within cities, can be comparable to natural systems (Davies et al., 2013). Our estimates of carbon density, especially those per unit of treed area, show that these values in Brisbane can equal or exceed values in nearby natural and managed ecosystems. Estimates from the Karawatha urban forest located within Brisbane (147 MgC ha^{-1}; Hero et al., 2013) and nearby Stradbroke Island (180 MgC ha^{-1}; Westman and Rogers, 1977) are very similar to our estimates for nature conservation, resource protection, and plantation land uses within Brisbane (130–160 MgC ha^{-1}). Similarly, our values from utility, residential, transportation, and industrial areas (89–113 MgC ha^{-1}) are larger than other estimates for eucalyptus woodlands in Queensland (44 MgC ha^{-1}; Burrows et al., 2002) and monoculture and mixed plantation forests in Queensland and northern New South Wales (60–85 MgC ha^{-1}, Kanowski and Catterall, 2010; 30–57 MgC ha^{-1}, Specht and West, 2003). The levels of carbon density that we observed and estimate across Brisbane emphasize the importance of more accurately quantifying urban carbon stocks and understanding how urbanization drives changes in aboveground carbon in order to inform policy and planning.

Our values of carbon density are somewhat higher than other estimates of urban carbon density around the world, but not exceptionally so. We estimated that the mean urban carbon density across the urban land area of Brisbane was 32.6 ± 5.8 MgC ha^{-1} with this value increasing to 110.9 ± 19.7 MgC ha^{-1} when considering only treed areas. While these values are somewhat higher than those from the oft-cited Nowak and Crane (2002) of 25.1 MgC ha^{-1} across ten U.S. cities, they match more closely with a recent study of cities in Wisconsin which range from 12 to 56 MgC ha^{-1} (Gu and Townsend, 2017). In addition, there is wide variation in reported urban carbon densities. Davies et al. (2013) found values that ranged from 5 to 89 MgC ha^{-1} overall for urban areas and 7–290 MgC ha^{-1} for urban forest cover across thirteen urban studies. Similarly, across 34 US cities carbon storage densities ranged from 31 to 141 MgC ha^{-1} (Nowak et al., 2013). While most of this variation between studies likely arises from variation in the tree cover per hectare of land across cities, some is also due to inconsistent methods in how urban areas are defined and delineated and how carbon stores are quantified, making it difficult to compare results across studies and cities (Davies et al., 2011, 2013). Subtropical moist forests, especially those in Australia, also have some of the highest aboveground carbon stocks in the world with average values of 294 MgC ha^{-1} worldwide compared to cool temperate rainforests (377 MgC ha^{1}) or tropical wet (171 MgC ha^{-1}) or moist (179 MgC ha^{-1}) forests (Keith et al., 2009). In part, this may be due to the dense wood of the *Eucalyptus* (mean: 0.828 g cm^{-3}) and *Casuarina* (mean: 0.839 g cm^{-3}) trees that dominate Brisbane's forests relative to tree species in the temperate zone cities that have been the focus of most other studies (e.g., *Crataegus*: 0.794; *Fraxinus*: 0.568; *Acer*: 0.540; *Prunus*: 0.589; *Pseudotsuga*: 0.461; *Tsuga*: 0.422; http://db.worldagroforestry.org/wd). Thus, for a given volume of wood, Brisbane's trees and forests likely contain more biomass and carbon per unit area than those in many other cities. In addition, the urban area of Brisbane has higher canopy cover (27%) than most other cities that have been investigated for carbon stocks (Jacobs et al., 2014). Out of the thirteen studies examined by Davies et al. (2013), only four cities (Gainesville, Boston, Xiamen, and Atlanta) had greater tree cover than Brisbane. Thus, the relatively high values for Brisbane are most likely due to a combination of the highly productive sub-tropical forests that consist of tree species with dense wood and the city's high vegetation cover.

Finally, the high spatial resolution of our analysis may have also contributed to higher estimated carbon stocks than found in other studies by allowing us to capture small patches of vegetation and individual trees across the city. Cities are incredibly complex and heterogeneous landscapes where vegetation is often present as very small patches or even scattered trees (Cadenasso et al., 2007; Gill et al., 2008). As land cover data becomes coarser, these small, vegetated features are lost, as is their contribution to carbon stores. In other words, coarse data often fail to accurately represent the fine-grained pattern of urban systems (Davies et al., 2013; Bottalico et al., 2017). These types of effects of the spatial resolution of data have well known effects in landscape ecology (Lechner and Rhodes, 2016). The consequences of this for carbon stores are significant. An analysis in Leicester, UK, found that moving from 10 m to 250 m resolution land cover data meant a 73% underestimate of aboveground carbon stores (Davies et al., 2013).

4.4. Implications for urban planning and land use management

The implications of a relationship between landscape structure and carbon storage, and to a lesser extent between urban form and carbon storage, with respect to our understanding of the effects of urbanization on carbon are significant. While limiting urban spread and land clearing are critical to minimize the effects of urbanization on aboveground carbon stocks, our results also suggest that targeted management of aboveground carbon stocks in the most fragmented areas of urban landscapes, as calculated at contrasting fine (1 ha) and broad (1 km^2) spatial scales, could also help increase urban carbon stores. For example, by planting tree species that store more carbon (e.g., greater wood density, taller trees) in these areas, purposefully managing trees in fragmented urban areas to increase vertical complexity and maximize carbon stores per unit area, or promoting the protection of older or larger trees that store a disproportionate amount of carbon in the more fragmented portions of cities. If the edge effects important in natural forests are also important in urban forests and influence carbon stores, then actively managing urban landscape structure (e.g., clumping patches of trees together, limiting development to minimize forest fragmentation) could also be a tool to increase urban carbon stocks. However, this depends on first determining if these landscape carbon relationships are widespread in cities, and then connecting these landscape patterns to the underlying mechanisms that link urban landscape structure to carbon stocks.

It is also important to note that the carbon stores quantified here are not permanent, but are in continual flux as vegetation dies or is cleared and releases carbon to the atmosphere, and trees are planted or new growth sequesters it (Nowak and Crane, 2002). This is especially important in urban areas, where in most locations natural regrowth is not possible and human planting of vegetation is necessary (Rowntree and Nowak, 1991). How changes in urban landscape structure through time might affect these processes is an open question that requires further research. Our methods for quantifying urban carbon stores, by coupling remotely sensed LiDAR data with field studies provides a way forward for monitoring urban carbon through time. It is becoming more common for cities to institute regular LiDAR sampling, which, if coupled with regular field sampling of aboveground carbon could

provide a relatively easy way to monitor urban carbon stocks through time. This will especially be the case if cities begin to collect LiDAR data at higher pulse densities than is currently common, which would allow more accurate quantification of vegetation structural metrics. By incorporating permanent field plots into such a system, measures of carbon sequestration and loss as urbanization proceeds could then be quantified. Such a monitoring program would significantly improve our understanding of how urbanization affects carbon stocks and how to best design cities to maximize these stocks.

Finally, urbanization and changes in urban form do not solely impact carbon, but also have effects on multiple ecosystem processes, ecosystem services, and social processes. Changes to urban landscape structure and vegetation structure are likely to impact urban heat island mitigation by vegetation, recreational opportunities in green spaces, flood and air quality regulation, human health, and biodiversity. How these different ecosystem services interact with carbon storage as urban landscape structure changes needs to be quantified if truly multifunctional urban landscapes are to be realized. The impacts that changes to urban form may also have on carbon emissions, such as from additional building heating costs, transportation, and management of vegetation (e.g., mowing, pruning, etc.) also need to be explored to ensure that measures to store more carbon in urban areas do not lead to increased emissions. An additional concern, especially in Australia, is how changes to vegetation and landscape structure may impact wildfire risk (Eriksen and Head, 2014). As Hutyra et al. (2011) note, cities are tightly coupled human-natural systems that exhibit nonlinearities, thresholds, and fuzzy boundary conditions that will make it challenging to manage them for carbon, other ecosystem services, and human wellbeing simultaneously.

5. Conclusions

Our study provides new and important evidence that urbanization's effects on carbon are not only related to changes in land use and the total amount of vegetation present across cities, but also arise from the landscape-scale fragmentation of urban vegetation and how this affects the fine-scale vertical structure of urban vegetation. Our results therefore emphasize the need to better understand and identify the important drivers of landscape-scale variation in urban carbon, what the specific ecological and socioecological mechanisms are that underlie these patterns, and how to use this understanding to inform management and policies in cities to increase carbon stocks. In particular, our results demonstrate that management of urban vegetation aimed at increasing carbon stocks should focus on the most fragmented areas of the city and how to increase carbon densities in these areas. Understanding the distribution and key drivers of urban carbon stocks across spatial scales will become increasingly important as the world's population becomes increasingly urbanized and the need for cities to reduce and mitigate their carbon emissions intensifies.

Acknowledgments

We thank Brisbane City Council, the Queensland Government, and the Australia Commonwealth Government for providing the data necessary for this study. Caroline Tan, Janine Jones, Andrés Felipe Suarez-Castro, Nathalie Butt, Claire Runge, Marie Dade, Sarah Chapman, Rhiannon Caynes, and Yang Zhou assisted in fieldwork; John Dwyer provided invaluable plant identification expertise. This work was supported by the Australian Research Council Discovery Project DP130100218.

Appendix A. Supplementary data

Supplementary data to this article can be found online at https://doi.org/10.1016/j.scitotenv.2017.11.255.

References

ABARES, 2016. The Australian Land Use and Management Classification Version 8. Australian Bureau of Agricultural and Resource Economics and Sciences, Canberra, CC BY. 3.0.
ABOM, 2016. Brisbane Historical Climate Data. Australian Bureau of Meteorology Available at:. http://www.bom.gov.au/climate/data/ (accessed 16.10.19).
Accad, A., Neldner, V.J., 2015. Remnant Regional Ecosystem Vegetation in Queensland, Analysis 1997–2013. Queensland Department of Science, Information Technology and Innovation, Brisbane, Australia.
Alonzo, M., Bookhagen, B., McFadden, J.P., Sun, A., Roberts, D.A., 2015. Mapping urban forest leaf area index with airborne lidar using penetration metrics and allometry. Remote Sens. Environ. 162, 141–153.
Alonzo, M., McFadden, J.P., Nowak, D.J., Roberts, D.A., 2016. Mapping urban forest structure and function using hyperspectral imagery and LiDAR data. Urban For. Urban Green. 17 (1), 135–147.
Armston, J.D., Denham, R.J., Danaher, T., Scarth, P.F., Moffiet, T.N., 2009. Prediction and validation of foliage projective cover from Landsat-5 TM and Landsat-7 ETM+ imagery. J. Appl. Remote. Sens. 3, 033540.
Asner, G.P., Powell, G.V.N., Mascaro, J., Knapp, D.E., Clark, J.K., Jacobson, J., Kennedy-Bowdoin, T., Balaji, A., Paez-Acosta, G., Victoria, E., Secada, L., Valqui, M., Hughes, R.F., 2010. High-resolution forest carbon stocks and emissions in the Amazon. Proc. Natl. Acad. Sci. 107 (38), 16,738–16,742.
Asner, G.P., Knapp, D.E., Martin, R.E., Tupayachi, R., Anderson, C.B., Mascaro, J., Sinca, F., Chadwick, K.D., Higgins, M., Farfan, W., Llactayo, W., Silman, M.R., 2014. Targeted carbon conservation at national scales with high-resolution monitoring. Proc. Natl. Acad. Sci. 111 (47), E5016–E5022.
Bartón, K., 2013. Package "MuMIn": Multi-Model Inference.
Baskerville, G.L., 1972. Use of logarithmic regression in the estimation of plant biomass. Can. J. For. Res. 2, 49–53.
Beckmann, G.G., Hubble, G.D., Thompson, C.H., 1987. The soil landscapes of Brisbane and south-eastern environs. CSIRO Soils and Land Use Series No. 60. Melbourne, Australia.
Bivand, R., Altman, M., Anselin, L., Assunção, R., Berke, O., Bernat, A., et al., 2015. Package "spdep" - Spatial Dependence: Weighting Scheme, Statistics and Models. R.
Bottalico, F., Travaglini, D., Chirici, G., Garfì, V., Giannetti, F., De Marco, A., Fares, S., Marchetti, M., Nocentini, S., Paoletti, E., Salbitano, F., Sanesi, G., 2017. A spatially-explicit method to assess the dry deposition of air pollution by urban forests in the city of Florence, Italy. Urban For. Urban Green. 27, 221–234.
Burrows, W.H., Henry, B.K., Back, P.V., Hoffmann, M.B., Tait, L.J., Anderson, E.R., Menke, N., Danaher, T., Carter, J.O., McKeon, G.M., 2002. Growth and carbon stock change in eucalypt woodlands in northeast Australia: ecological and greenhouse sink implications. Glob. Chang. Biol. 8, 769–784.
Buston, P.M., Elith, J., 2011. Determinants of reproductive success in dominant pairs of clownfish: a boosted regression tree analysis. J. Anim. Ecol. 80 (3), 528–538.
Cadenasso, M.L., Pickett, S.T.A., Schwarz, K., 2007. Spatial heterogeneity in urban ecosystems: reconceptualizing land cover and a framework for classification. Front. Ecol. Environ. 5 (2), 80–88.
Caynes, R.J.C., Mitchell, M.G., Wu, D., Johansen, K., Rhodes, J.R., 2016. Using high-resolution LiDAR data to quantify the three-dimensional structure of vegetation in urban green space. Urban Ecosyst. 19 (4), 1749–1765.
Chaplin-Kramer, R., Ramler, I., Sharp, R., Haddad, N.M., Gerber, J.S., West, P.C., Mandle, L., Engstrom, P., Baccini, A., Sim, S., Mueller, C., King, H., 2015. Degradation in carbon stocks near tropical forest edges. Nat. Commun. 6, 10,158.
Chave, J., Andalo, C., Brown, S., Cairns, M.A., Chambers, J.Q., Eamus, D., Fölster, H., Fromard, F., Higuchi, N., Kira, T., Lescure, J.-P., Nelson, B.W., Ogawa, H., Puig, H., Riéra, B., Yamakura, T., 2005. Tree allometry and improved estimation of carbon stocks and balance in tropical forests. Oecologia 145 (1), 87–99.
Churkina, G., Brown, D.G., Keoleian, G., 2010. Carbon stored in human settlements: the conterminous United States. Glob. Chang. Biol. 16 (1), 135–143.
Damschen, E., Haddad, N.M., Orrock, J.L., Tewksbury, J.J., Levey, D.J., 2006. Corridors increase plant species richness at large scales. Science 313 (5791), 1284–1286.
Davies, A.B., Asner, G.P., 2014. Advances in animal ecology from 3D-LiDAR ecosystem mapping. Trends Ecol. Evol. 29 (12), 681–691.
Davies, Z.G., Edmondson, J., Heinemeyer, A., Leake, J.R., Gaston, K.J., 2011. Mapping an urban ecosystem service: quantifying above-ground carbon storage at a city-wide scale. J. Appl. Ecol. 48 (5), 1125–1134.
Davies, Z.G., Dallimer, M., Edmondson, J., Leake, J.R., Gaston, K.J., 2013. Identifying potential sources of variability between vegetation carbon storage estimates for urban areas. Environ. Pollut. 183, 133–142.
Department of Science, Information Technology and Innovation, 2014. Land Cover Change in the South East Queensland Region 2012–2014. https://publications.qld.gov.au/dataset/8d2f982c-7a5b-41fa-935e-5f0ea4f65f9a/resource/5f4c2910-a93f-4c53-8b2c-fbf655631f16/download/southeastqld201214.pdf (accessed 16.11.14).
Dhakal, S., 2010. GHG emissions from urbanization and opportunities for urban carbon mitigation. Curr. Opin. Environ. Sustain. 2 (4), 277–283.
Dormann, C.F., McPherson, J.M., Araújo, M.B., Bivand, R., Bolliger, J., Carl, G., Davies, R.G., Hirzel, A., Jetz, W., Kissling, W.D., Kühn, I., Ohlemüller, R., Peres-Neto, R., Reineking, B., Schröder, B., Schurr, F.M., Wilson, R., 2007. Methods to account for spatial autocorrelation in the analysis of species distributional data: a review. Ecography 30 (5), 609–628.
Drake, J.B., Dubayah, R.O., Clark, D.B., Knox, R.G., Blair, J.B., Hofton, M.A., Chazdon, R.L., Weishampel, J.F., Prince, S.D., 2002. Estimation of tropical forest structural characteristics using large-footprint lidar. Remote Sens. Environ. 79 (2), 305–319.
Ediriweera, S., Pathirana, S., Danaher, T., Nichols, D., 2014. Estimating above-ground biomass by fusion of LiDAR and multispectral data in subtropical woody plant communities in topographically complex terrain in North-eastern Australia. J. For. 25, 761–771.

Edmondson, J., Davies, Z.G., McHugh, N., Gaston, K.J., Leake, J.R., 2012. Organic carbon hidden in urban ecosystems. Sci. Rep. 2, 963.
Elith, J., Leathwick, J.R., Hastie, T., 2008. A working guide to boosted regression trees. J. Anim. Ecol. 77 (4), 802–813.
Eriksen, C., Head, L., 2014. Geographical fire research in Australia: review and prospects. Geogr. Res. 52 (1), 1–5.
van Ewijk, K.Y., Randin, C.F., Treitz, P.M., Scott, N.A., 2014. Predicting fine-scale tree species abundance patterns using biotic variables derived from LiDAR and high spatial resolution imagery. Remote Sens. Environ. 150, 120–131.
Fragkias, M., Güneralp, B., Seto, K.C., Goodness, J., 2013. A synthesis of global urbanization projections. In: Elmgvist, T., Fragkias, M., Goodness, J., Güneralp, B., Marcotullio, P.J., McDonald, R.I., et al. (Eds.), Urbanization, Biodiversity and Ecosystem Services Challenges and Opportunities A Global Assessment. Springer, Netherlands, Dordrecht, pp. 409–435.
Garćia-Gutiérrez, J., Martínez-Álvarez, F., Troncoso, A., Riquelme, J.C., 2015. A comparison of machine learning regression techniques for LiDAR-derived estimation of forest variables. Neurocomputing 167, 24–31.
Garden, J.G., McAlpine, C.A., Possingham, H.P., Jones, D.N., 2007. Habitat structure is more important than vegetation composition for local-level management of native terrestrial reptile and small mammal species living in urban remnants: a case study from Brisbane, Australia. Austral Ecol. 32 (6), 669–685.
Gaston, K.J., Ávila-Jiménez, M.L., Edmondson, J., 2013. Managing urban ecosystems for goods and services. J. Appl. Ecol. 50 (4), 830–840.
Gelman, A., Su, Y.-S., Ya-jima, M., Hill, J., Grazia Pittau, M., Kerman, J., et al., 2013. Package "Arm": Data Analysis Using Regression and Multilevel/Hierarchical Models.
Gill, S.E., Handley, J.F., Ennos, A.R., Pauleit, S., Theuray, N., Lindley, S.J., 2008. Characterising the urban environment of UK cities and towns: a template for landscape planning. Landsc. Urban Plan. 87 (3), 210–222.
Godwin, C., Chen, G., Singh, K.K., 2015. The impact of urban residential development patterns on forest carbon density: an integration of LiDAR, aerial photography and field mensuration. Landsc. Urban Plan. 136, 97–109.
Goodwin, N.R., Coops, N.C., Tooke, T.R., Christen, A., Voogt, J.A., 2009. Characterizing urban surface cover and structure with airborne lidar technology. Can. J. Remote. Sens. 35 (3), 297–309.
Grimm, N.B., Faeth, S.H., Golubiewski, N.E., Redman, C.L., Wu, J., Bai, X., Briggs, J.M., 2008. Global change and the ecology of cities. Science 319 (5864), 756–760.
Gu, H., Townsend, P.A., 2017. Mapping forest structure and uncertainty in an urban area using leaf-off LiDAR data. Urban Ecosyst. 20 (2), 497–509.
Harper, K.A., Macdonald, S.E., Burton, P.J., 2005. Edge influence on forest structure and composition in fragmented landscapes. Conserv. Biol. 19 (3), 768–782.
Hastie, T.J., Tibshirani, R.J., Friedman, J.H., 2011. The Elements of Statistical Learning: Data Mining, Inference, and Prediction. Springer, New York.
Hero, J.-M., Castley, J.G., Butler, S.A., Lollback, G.W., 2013. Biomass estimation within an Australian eucalypt forest: meso-scale spatial arrangement and the influence of sampling intensity. For. Ecol. Manage. 310, 547–554.
Höfle, B., Hollaus, M., Hagenauer, J., 2012. Urban vegetation detection using radiometrically calibrated small-footprint full-waveform airborne LiDAR data. ISPRS J. Photogramm. Remote Sens. 67, 134–147.
Hunt, A., Watkiss, P., 2011. Climate change impacts and adaptation in cities: a review of the literature. Clim. Change 104 (1), 13–49.
Hutyra, L.R., Yoon, B., Alberti, M., 2011. Terrestrial carbon stocks across a gradient of urbanization: a study of the Seattle, WA region. Glob. Chang. Biol. 17 (2), 783–797.
Imhoff, M.L., Bounoua, L., Ricketts, T.H., Loucks, C., Harriss, R., Lawrence, W.T., 2004. Global patterns in human consumption of net primary production. Nature 429 (6994), 870–873.
Jacobs, B., Mikhailovich, N., Moy, C., 2014. Benchmarking Australia's Urban Tree Canopy: an i-Tree Assessment, Final Report. Institute for Sustainable Futures, University of Technology Sydney, Sydney, pp. 1–47.
Jaskierniak, D., Lane, P.N., Robinson, A., Lucieer, A., 2011. Extracting LiDAR indices to characterise multilayered forest structure using mixture distribution functions. Remote Sens. Environ. 115 (2), 573–585.
Kanowski, J., Catterall, C.P., 2010. Carbon stocks in above-ground biomass of monoculture plantations, mixed species plantations and environmental restoration plantings in north-east Australia. Ecol. Manage. Restor. 11 (2), 119–126.
Keith, H., Mackey, B.G., Lindenmayer, D.B., 2009. Re-evaluation of forest biomass carbon stocks and lessons from the world's most carbon-dense forests. Proc. Natl. Acad. Sci. U. S. A. 106 (28), 11,635–11,640.
Kennedy, K.A., Addison, P.A., 1987. Some considerations for the use of visual estimates of plant cover in biomonitoring. J. Ecol. 75 (1), 151.
Leathwick, J.R., Elith, J., Francis, M.P., Hastie, T., Taylor, P., 2006. Variation in demersal fish species richness in the oceans surrounding New Zealand: an analysis using boosted regression trees. Mar. Ecol. Prog. Ser. 321, 267–281.
Lechner, A.M., Rhodes, J.R., 2016. Recent progress on spatial and thematic resolution in landscape ecology. Current Landscape Ecology Reports. 1, pp. 98–105.
Lefsky, M.A., Cohen, W.B., Harding, D.J., Parker, G.G., Acker, S.A., Gower, S.T., 2002a. Lidar remote sensing of above-ground biomass in three biomes. Glob. Ecol. Biogeogr. 11 (5), 393–399.
Lefsky, M.A., Cohen, W.B., Parker, G.G., Harding, D.J., 2002b. Lidar remote sensing for ecosystem studies. BioScience 52 (1), 19–30.
Li, M., Im, J., Quackenbush, L.J., Liu, T., 2014. Forest biomass and carbon stock quantification using airborne LiDAR data: a case study over Huntington wildlife forest in the Adirondack park. IEEE Journal of Selected Topics in Applied Earth Observation and Remote Sensing 7 (7), 3134–3156.
Lieb, M., Schmidt, J., Glaser, B., 2016. Improving the spatial prediction of soil organic carbon stocks in a complex tropical mountain landscape by methodological specifications in machine learning approaches. PLoS One 11 (4), e0153673.
Lovell, J.L., Jupp, D.L., Culvenor, D.S., Coops, N.C., 2003. Using airborne and ground-based ranging LiDAR to measure canopy structure in Australian forests. Can. J. Remote. Sens. 29 (5), 607–622.
Ma, J., Xiao, X., Qin, Y., Chen, B., Hu, Y., Li, X., Zhao, B., 2017. Estimating aboveground biomass of broadleaf, needleleaf, and mixed forests in Northeastern China through analysis of 25-m ALOS/PALSAR mosaic data. For. Ecol. Manage. 389, 199–210.
McCarthy, M.P., Best, M.J., Betts, R.A., 2010. Climate change in cities due to global warming and urban effects. Geophys. Res. Lett. 37 (9), L09705.
Mcdonald, R.I., Kareiva, P.M., Forman, R.T.T., 2008. The implications of current and future urbanization for global protected areas and biodiversity conservation. Biol. Conserv. 141 (6), 1695–1703.
McGarigal, K., Cushman, S., Ene, E., 2012. FRAGSTATS v4.2: Spatial Pattern Analysis Program for Categorical Maps. University of Massachusetts, Amherst http://www.umass.edu/landeco/research/fragstats/fragstats.html (accessed 16.10.30).
McHale, M.R., Burke, I.C., Lefsky, M.A., Peper, P.J., 2009. Urban forest biomass estimates: is it important to use allometric relationships developed specifically for urban trees? Urban Ecosyst. 12, 95–113.
Mitchell, M.G., Wu, D., Johansen, K., Maron, M., McAlpine, C., Rhodes, J.R., 2016. Landscape structure influences urban vegetation vertical structure. J. Appl. Ecol. 53, 1477–1488.
Miura, N., Jones, S.D., 2010. Characterizing forest ecological structure using pulse types and heights of airborne laser scanning. Remote Sens. Environ. 114 (5), 1069–1076.
Nagelkerke, N., 1991. A note on a general definition of the coefficient of determination. Biometrika 78 (3), 691–692.
Nowak, D.J., 1993. Atmospheric carbon-reduction by urban trees. J. Environ. Manage. 37 (3), 207–217.
Nowak, D.J., 1994. Atmospheric carbon dioxide reduction by Chicago's urban forest. In: McPherson, E.G., Nowak, D.J., Rowntree, R.A. (Eds.), Chicago's Urban Forest Ecosystem: Results of the Chicago Urban Forest Climate Project. United States Department of Agriculture, Forest Service, Northeastern Forest Experimental Station, General Technical Report NE-186, Radnor, PA, pp. 83–94.
Nowak, D.J., Crane, D.E., 2002. Carbon storage and sequestration by urban trees in the USA. Environ. Pollut. 116 (3), 381–389.
Nowak, D.J., Greenfield, E.J., Hoehn, R.E., Lapoint, E., 2013. Carbon storage and sequestration by trees in urban and community areas of the United States. Environ. Pollut. 178, 229–236.
Pütz, S., Groeneveld, J., Henle, K., Knogge, C., Martensen, A.C., Metz, M., Metzger, J.P., Ribeiro, M.C., Dantas de Paula, M., Huth, A., 2014. Long-term carbon loss in fragmented Neotropical forests. Nat. Commun. 5, 5037.
QGSO, 2015. Population Growth Highlights and Trends, Queensland Regions. 2015 edition. Queensland Government Statistician's Office, Queensland Treasury, City East, Australia.
Queensland Government, 2011. Queensland Government Population Projections to 2031 - Local Government Areas. Queensland Treasury, City East, Australia.
Raciti, S.M., Hutyra, L.R., Rao, P., Finzi, A.C., 2012. Inconsistent definitions of "urban" result in different conclusions about the size of urban carbon and nitrogen stocks. Ecol. Appl. 22 (3), 1015–1035.
Raciti, S.M., Hutyra, L.R., Newell, J.D., 2014. Mapping carbon storage in urban trees with multi-source remote sensing data: Relationships between biomass, land use, and demographics in Boston neighborhoods. Sci. Total Environ. 500–501, 72–83.
Razakamanarivo, R.H., Grinand, C., Antoinette, M.R., Bernoux, M., Albrecht, A., 2011. Mapping organic carbon stocks in eucalyptus plantations of the central highlands of Madagascar: a multiple regression approach. Geoderma 162 (3–4), 335–346.
Remy, E., Wuyts, K., Boeckx, P., Ginzburg, S., Gundersen, P., Demey, A., Van Den Buicke, J., Van Acker, J., Verheyen, K., 2016. Strong gradients in nitrogen and carbon stocks at temperate forest edges. For. Ecol. Manage. 376, 45–58.
Richardson, J.J., Moskal, L.M., Kim, S.-H., 2009. Modeling approaches to estimate effective leaf area index from aerial discrete-return LiDAR. Agric. For. Meteorol. 149 (6–7), 1152–1160.
Ridgeway, G., 2015. Package "gbm": Generalized Boosted Regression Models.
Rowntree, R.A., Nowak, D.J., 1991. Quantifying the role of urban forests in removing atmospheric carbon dioxide. J. Arboric. 17 (10), 269–275.
Seto, K.C., Güneralp, B., Hutyra, L.R., 2012. Global forecasts of urban expansion to 2030 and direct impacts on biodiversity and carbon pools. Proc. Natl. Acad. Sci. U. S. A. 109 (40), 16,083–16,088.
Shrestha, R., Wynne, R.H., 2012. Estimating biophysical parameters of individual trees in an urban environment using small footprint discrete-return imaging Lidar. Remote Sens. 4 (12), 484–508.
Simonson, W.D., Allen, H.D., 2014. Applications of airborne lidar for the assessment of animal species diversity. Methods Ecol. Evol. 5, 719–729.
Specht, A., West, P.W., 2003. Estimation of biomass and sequestered carbon on farm forest plantations in northern New South Wales, Australia. Biomass Bioenergy 25, 363–379.
Strohbach, M.W., Haase, D., 2012. Above-ground carbon storage by urban trees in Leipzig, Germany: Analysis of patterns in a European city. Landsc. Urban Plan. 104 (1), 95–104.
Tanhuanpää, T., Vastaranta, M., Kankare, V., Holopainen, M., Hyppä, J., Hyppä, H., Alho, P., Raisio, J., 2014. Mapping of urban roadside trees - a case study in the tree regisdter update process in Helsinki City. Urban For. Urban Green. 13 (3), 562–570.
Tigges, J., Churkina, G., Lakes, T., 2017. Modeling above-ground carbon storage: a remote sensing approach to derive individual tree species information in urban settings. Urban Ecosyst. 20 (1), 97–111.
Tooke, T.R., Coops, N.C., Goodwin, N.R., Voogt, J.A., 2009. Extracting urban vegetation characteristics using spectral mixture analysis and decision tree classifications. Remote Sens. Environ. 113, 398–407.
Trombulak, S.C., Frissell, C.A., 2000. Review of ecological effects of roads on terrestrial and aquatic communities. Conserv. Biol. 14 (1), 18–30.

United Nations, 2014. World Urbanization Prospects: The 2014 Revision, Highlights. United Nations, Department of Economic and Social Affairs, Population Division, New York, NY.

United Nations, 2015. World Population Prospects: The 2015 Revision, Key Findings and Advance Tables. United Nations, Department of Economic and Social Affairs, Population Division, New York, NY.

Varhola, A., Coops, N.C., 2013. Estimation of watershed-level distributed forest structure metrics relevant to hydrologic modeling using LiDAR and Landsat. J. Hydrol. 487, 70–86.

Velasco, E., Roth, M., Tan, S.H., Quak, M., Nabarro, S.D.A., Norford, L., 2013. The role of vegetation in the CO2 flux from a tropical urban neighbourhood. Atmos. Chem. Phys. 13 (10), 185–10,202.

Westman, W.E., Rogers, R.W., 1977. Biomass and structure of a subtropical eucalypt forest, North Stradbroke Island. Aust. J. Bot. 25, 171–191.

Ziter, C., Bennett, E.M., Gonzalez, A., 2014. Temperate forest fragments maintain aboveground carbon stocks out to the forest edge despite changes in community composition. Oecologia 176 (3), 893–902.